EUROPEAN ORGANIZATION FOR NUCLEAR RESEARCH (CERN)

CERN-EP-2016-082
LHCb-PAPER-2016-010
2 June 2016

Measurement of the properties of the Ξ_b^{*0} baryon

The LHCb collaboration[†]

Abstract

We perform a search for near-threshold Ξ_b^0 resonances decaying to $\Xi_b^-\pi^+$ in a sample of proton-proton collision data corresponding to an integrated luminosity of $3\,\text{fb}^{-1}$ collected by the LHCb experiment. We observe one resonant state, with the following properties:

$$\begin{aligned} m(\Xi_b^{*0}) - m(\Xi_b^-) - m(\pi^+) &= 15.727 \pm 0.068\,(\text{stat}) \pm 0.023\,(\text{syst})\ \text{MeV}/c^2, \\ \Gamma(\Xi_b^{*0}) &= 0.90 \pm 0.16\,(\text{stat}) \pm 0.08\,(\text{syst})\ \text{MeV}. \end{aligned}$$

This confirms the previous observation by the CMS collaboration. The state is consistent with the $J^P = 3/2^+$ Ξ_b^{*0} resonance expected in the quark model. This is the most precise determination of the mass and the first measurement of the natural width of this state. We have also measured the ratio

$$\frac{\sigma(pp \to \Xi_b^{*0} X)\mathcal{B}(\Xi_b^{*0} \to \Xi_b^-\pi^+)}{\sigma(pp \to \Xi_b^- X)} = 0.28 \pm 0.03\,(\text{stat}) \pm 0.01\,(\text{syst}).$$

Published as JHEP 1605 (2016) 161.

[†]Authors are listed at the end of this paper.

1 Introduction

Precise measurements of the properties of hadrons provide important metrics by which models of quantum chromodynamics (QCD), including lattice QCD and potential models employing the symmetries of QCD, can be tested. Studies of hadrons containing a heavy quark play a special role since the heavy quark symmetry can be exploited, for example to relate properties of charm hadrons to beauty hadrons. Measurements of the masses and mass splittings between the ground and excited states of beauty and charm hadrons provide a valuable probe of the interquark potential [1].

There are a number of b baryon states that contain both beauty and strange quarks. The singly strange states form isodoublets: Ξ_b^0 (bsu) and Ξ_b^- (bsd). Theoretical estimates of the properties of these states are available (see, *e.g.*, Refs. [1–12]). There are five known Ξ_b states which, in the constituent quark model, correspond to five of the six low-lying states that are neither radially nor orbitally excited: one isodoublet of weakly-decaying ground states (Ξ_b^0 and Ξ_b^-) with $J^P = \frac{1}{2}^+$, one isodoublet ($\Xi_b^{\prime 0}$ and $\Xi_b^{\prime -}$) with $J^P = \frac{1}{2}^+$ but different symmetry properties from the ground states, and one isodoublet (Ξ_b^{*0} and Ξ_b^{*-}) with $J^P = \frac{3}{2}^+$. The large data samples collected at the Large Hadron Collider have allowed these states to be studied in detail in recent years. These studies include precise measurements of the masses and lifetimes of the Ξ_b^0 and Ξ_b^- baryons [13, 14] by the LHCb collaboration, the observation of a peak in the $\Xi_b^-\pi^+$ mass spectrum interpreted as the Ξ_b^{*0} baryon [15] by the CMS collaboration, and the observation of two structures in the $\Xi_b^0\pi^-$ mass spectrum, consistent with the $\Xi_b^{\prime -}$ and Ξ_b^{*-} baryons [16] by LHCb.[1] The $\Xi_b^{\prime 0}$ state was not observed by CMS; it is assumed to be too light to decay into $\Xi_b^-\pi^+$.

In this paper, we present the results of a study of the $\Xi_b^-\pi^+$ mass spectrum, where the Ξ_b^- baryon is reconstructed through its decay to $\Xi_c^0\pi^-$, with $\Xi_c^0 \to pK^-K^-\pi^+$. The measurements use a pp collision data sample recorded by the LHCb experiment, corresponding to an integrated luminosity of $3\,\text{fb}^{-1}$, of which $1\,\text{fb}^{-1}$ was collected at $\sqrt{s} = 7\,\text{TeV}$ and $2\,\text{fb}^{-1}$ at $8\,\text{TeV}$. We observe a single peak in the $\Xi_b^-\pi^+$ mass spectrum, consistent with the state reported in Ref. [15]. A precise determination of its mass and the first determination of a non-zero natural width are reported. We also measure the relative production rate between the Ξ_b^{*0} and Ξ_b^- baryons in the LHCb acceptance.

The LHCb detector [17, 18] is a single-arm forward spectrometer covering the pseudorapidity range $2 < \eta < 5$, designed for the study of particles containing b or c quarks. The detector includes a high-precision tracking system consisting of a silicon-strip vertex detector surrounding the pp interaction region, a large-area silicon-strip detector located upstream of a dipole magnet with a bending power of about $4\,\text{Tm}$, and three stations of silicon-strip detectors and straw drift tubes placed downstream of the magnet. The tracking system provides a measurement of momentum, p, of charged particles with a relative uncertainty that varies from 0.5% at low momentum to 1.0% at $200\,\text{GeV}/c$. The minimum distance of a track to a primary vertex (PV), the impact parameter, is measured with a resolution of $(15 + 29/p_{\text{T}})\,\mu\text{m}$, where p_{T} is the component of the momentum transverse to the beam, in GeV/c. Different types of charged hadrons are distinguished

[1] Charge-conjugate processes are implicitly included throughout.

using information from two ring-imaging Cherenkov detectors. Photons, electrons and hadrons are identified by a calorimeter system consisting of scintillating-pad and preshower detectors, an electromagnetic calorimeter and a hadronic calorimeter. Muons are identified by a system composed of alternating layers of iron and multiwire proportional chambers. The online event selection is performed by a trigger [19], which consists of a hardware stage (L0), based on information from the calorimeter and muon systems, followed by a software stage, which applies a full event reconstruction. The software trigger requires a two-, three- or four-track secondary vertex which is significantly displaced from all primary pp vertices and for which the scalar $p_{\rm T}$ sum of the charged particles is large. At least one particle should have $p_{\rm T} > 1.7\,{\rm GeV}/c$ and be inconsistent with coming from any of the PVs. A multivariate algorithm [20] is used to identify secondary vertices consistent with the decay of a b hadron. Only events that fulfil these criteria are retained for this analysis.

In the simulation, pp collisions are generated using Pythia [21] with a specific LHCb configuration [22]. Decays of hadrons are described by EvtGen [23], in which final-state radiation is generated using Photos [24]. The interaction of the generated particles with the detector, and its response, are implemented using the Geant4 toolkit [25] as described in Ref. [26].

2 Candidate selection

Candidate Ξ_b^- decays are formed by combining $\Xi_c^0 \to pK^-K^-\pi^+$ and π^- candidates in a kinematic fit [27]. All tracks used to reconstruct the Ξ_b^- candidate are required to have good track fit quality, have $p_{\rm T} > 100\,{\rm MeV}/c$, and have particle identification information consistent with the hypothesis assigned. The large lifetime of the Ξ_b^- baryon is exploited to reduce combinatorial background by requiring all of its final-state decay products to have $\chi^2_{\rm IP} > 4$ with respect to all of the PVs in the event, where $\chi^2_{\rm IP}$, the impact parameter χ^2, is defined as the difference in the vertex fit χ^2 of the PV with and without the particle under consideration. The Ξ_c^0 candidates are required to have invariant mass within $20\,{\rm MeV}/c^2$ of the known value [28], corresponding to about three times the mass resolution. To further suppress background, the Ξ_b^- candidate must have a trajectory that points back to one of the PVs ($\chi^2_{\rm IP} \leq 10$) and must have a decay vertex that is significantly displaced from the PV with respect to which it has the smallest $\chi^2_{\rm IP}$ (decay time $> 0.2\,{\rm ps}$ and flight distance $\chi^2 > 100$). The invariant mass spectra of selected Ξ_c^0 and Ξ_b^- candidates are displayed in Fig. 1.

The Ξ_b^- candidates are then required to have invariant mass within $60\,{\rm MeV}/c^2$ of the peak value, corresponding to about four times the mass resolution. In a given event, each combination of Ξ_b^- and π^+ candidates is considered, provided that the pion has $p_{\rm T}$ greater than $100\,{\rm MeV}/c$ and is consistent with coming from the same PV as the Ξ_b^- candidate. The $\Xi_b^-\pi^+$ vertex is constrained to coincide with the PV in a kinematic fit, which is required to be of good quality. The $\Xi_b^-\pi^+$ system is also required to have $p_{\rm T} > 2.5\,{\rm GeV}/c$.

The mass difference δm is defined as

$$\delta m \equiv m_{\rm cand}(\Xi_b^-\pi^+) - m_{\rm cand}(\Xi_b^-) - m(\pi^+), \tag{1}$$

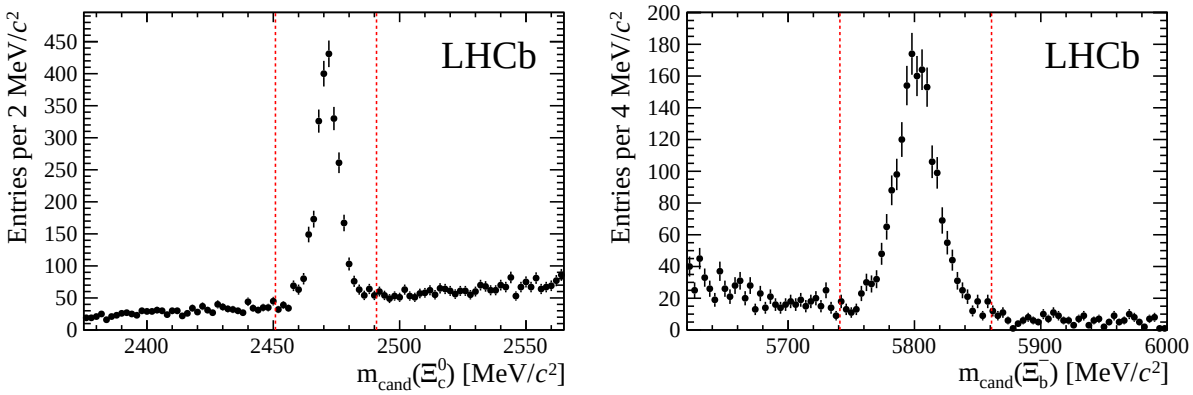

Figure 1: Mass spectra of (left) Ξ_c^0 and (right) Ξ_b^- candidates after all selection requirements are imposed, except for the one on the mass that is plotted. The vertical dashed lines show the selection requirements used in forming Ξ_b^- and Ξ_b^{*0} candidates.

where $m_{\rm cand}$ represents the reconstructed mass. The δm spectrum of $\Xi_b^-\pi^+$ candidates passing all selection requirements is shown in Fig. 2. A clear peak is seen at about $16\,\mathrm{MeV}/c^2$, whereas no such peak is seen in the wrong-sign ($\Xi_b^-\pi^-$) combinations, also shown in Fig. 2.

To determine the properties of the $\Xi_b^-\pi^+$ peak, we consider only candidates with $\delta m < 45\,\mathrm{MeV}/c^2$; this provides a large enough region to constrain the combinatorial background shape. There are on average 1.16 candidates per selected event in this mass region; all candidates are kept. In the vast majority of events with more than one candidate, a single Ξ_b^- candidate is combined with different π^+ tracks from the same PV.

3 Mass and width of $\Xi_b^-\pi^+$ peak

Accurate determination of the mass, width, and signal yield requires knowledge of the signal shape, and in particular the mass resolution. This is obtained from simulated Ξ_b^{*0} decays in which the δm value is set to the approximate peak location seen in data. In this simulation, the natural width of the $\Xi_b^-\pi^+$ state is fixed to a negligible value so that the shape of the distribution measured is due entirely to the mass resolution. The resolution function is parameterised as the sum of three Gaussian distributions with a common mean value. The weighted average of the three Gaussian widths is $0.51\,\mathrm{MeV}/c^2$. In the fits to data, all of the resolution shape parameters are fixed to the values obtained from simulation.

Any $\Xi_b^-\pi^+$ resonance in this mass region would be expected to have a non-negligible natural width Γ. The signal shape in fits to data is therefore described using a P-wave relativistic Breit–Wigner (RBW) line shape [29] with a Blatt–Weisskopf barrier factor [30], convolved with the resolution function described above.

The combinatorial background is modelled by an empirical threshold function of the

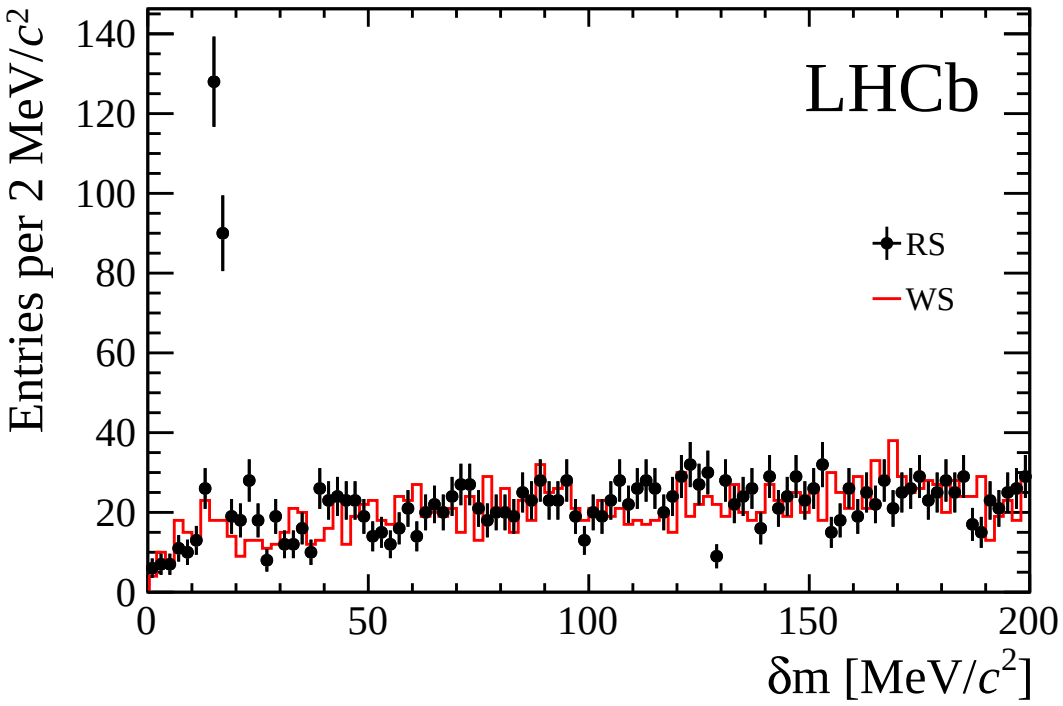

Figure 2: Distribution of δm. Right-sign candidates (RS, $\Xi_b^-\pi^+$) are shown as points with error bars, and wrong-sign candidates (WS, $\Xi_b^-\pi^-$) as a histogram. A single narrow structure is seen in the right-sign data.

form

$$f(\delta m) = \left(1 - e^{-\delta m/C}\right)\,(\delta m)^A, \tag{2}$$

where A and C are freely varying parameters determined in the fit to the data and δm is in units of MeV/c^2.

The mass, width and yield of events in the observed peak are determined from an unbinned, extended maximum likelihood fit to the δm spectrum using the signal and background shapes described above. The mass spectrum and the results of the fit are shown in Fig. 3. The fitted signal yield is 232 ± 19 events. The nonzero value of the natural width of the peak, $\Gamma = 0.90 \pm 0.16\,\text{MeV}$ (where the uncertainty is statistical only), is also highly significant: the change in log-likelihood when the width is fixed to zero exceeds 30 units. No other statistically significant structures are seen in the data.

We perform a number of cross-checks to ensure the robustness of the result. These include splitting the data by magnet polarity, requiring that one or more of the decay products of the signal candidate pass the L0 trigger requirements, dividing the data into subsamples in which the π^+ candidate has $p_{\rm T} < 250\,\text{MeV}/c$ and $p_{\rm T} > 250\,\text{MeV}/c$, varying the fit range in δm, and applying a multiple candidate rejection algorithm in which only

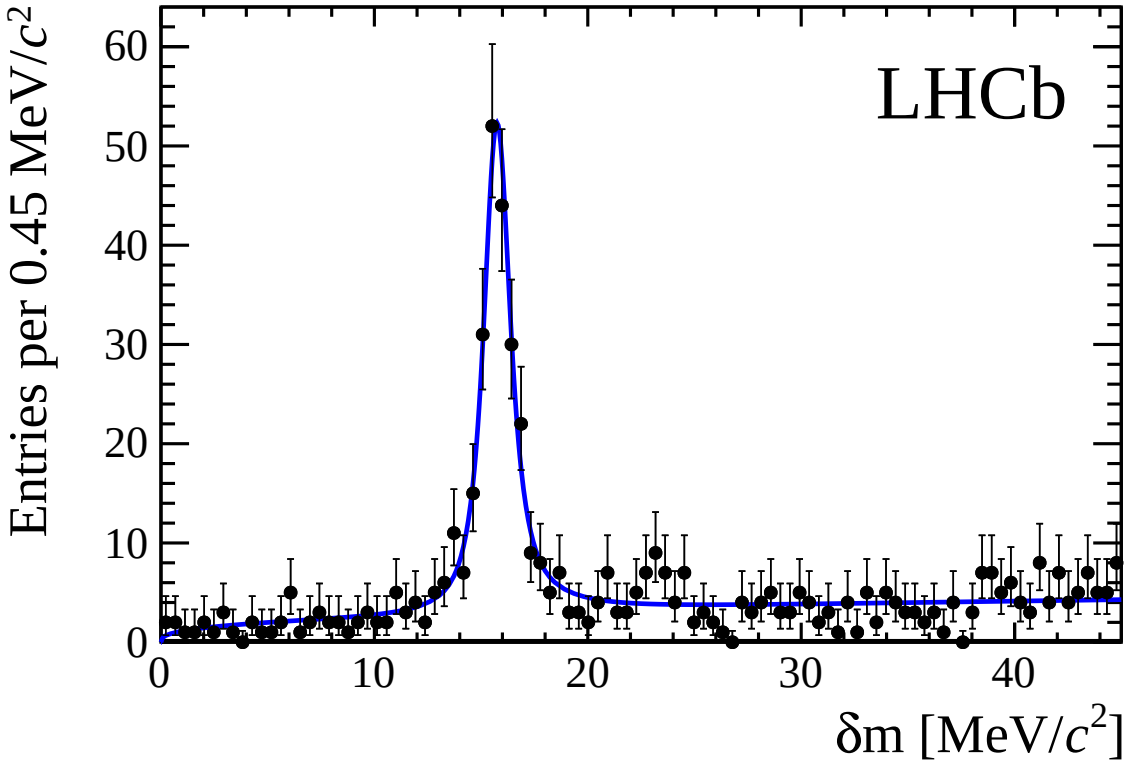

Figure 3: Distribution of δm along with the results of the fit described in the text.

one candidate, chosen at random, is retained in each event. In each of these cross-checks, the variation in fit results is consistent with statistical fluctuations.

Several sources of systematic effects are considered and are summarised in Table 1. Other than the first two systematic uncertainties described below, all are determined by making variations to the baseline selection or fit procedure, repeating the analysis, and taking the maximum change in δm or Γ. A small correction (16 keV, estimated with pseudoexperiments) to Γ is required due to the systematic underestimation of the width in a fit with limited yield; an uncertainty of the same size is assigned. This correction is already included in the value of Γ quoted earlier. The limited size of the sample of simulated events leads to uncertainties on the resolution function parameters. These uncertainties are propagated to the final results using the full covariance matrix. We assign a systematic uncertainty for a particular class of events with multiple Ξ_b^{*0} candidates in which the Ξ_b^- or Ξ_c^0 baryon is misreconstructed. This uncertainty is determined by applying a limited multiple candidate rejection procedure in which only one Ξ_b^0 candidate is accepted per event (but may be combined with multiple pions). The robustness of the resolution model is verified with control samples of $\Xi_b^{\prime -} \to \Xi_b^0 \pi^-$ (see Ref. [16]) and $D^{*+} \to D^0 \pi^+$; based on these tests, the uncertainty is assessed by increasing the Ξ_b^{*0} resolution width by 11%. This is the dominant uncertainty on Γ. An alternative background description is used in

the fit to check the dependence of the signal parameters on the background model. The calibration of the momentum scale has an uncertainty of 0.03% [31,32], the effect of which is propagated to the mass and width of the Ξ_b^{*0} baryon. As in Ref. [16], this is validated by measuring $m(D^{*+}) - m(D^0)$ in a large sample of D^{*+}, $D^0 \to K^-K^+$ decays. The mass difference agrees with a recent BaBar measurement [33] within $6\,\mathrm{keV}/c^2$, corresponding to 1.3σ when including the mass scale uncertainty for that decay. Finally, the dependence of the results on the relativistic Breit–Wigner lineshape is tested: other values of the assumed angular momentum (spin $0, 2$) and radial parameter (1–$5\,\mathrm{GeV}^{-1}$) of the Blatt–Weisskopf barrier factor are used, and an alternative parameterisation of the mass-dependent width (from appendix A of Ref. [29]) is tested.

Table 1: Systematic uncertainties, in units of MeV/c^2 (mass) and MeV (width).

Effect	δm	Γ
Fit bias correction		0.016
Simulated sample size	0.007	0.034
Multiple candidates	0.009	0.007
Resolution model	0.001	0.072
Background description	0.002	0.001
Momentum scale	0.009	0.001
RBW shape	0.017	0.011
Sum in quadrature	0.023	0.082
Statistical uncertainty	0.068	0.162

Taking these effects into account, the mass difference and width are measured to be

$$\begin{aligned} m(\Xi_b^{*0}) - m(\Xi_b^-) - m(\pi^+) &= 15.727 \pm 0.068 \pm 0.023\,\mathrm{MeV}/c^2, \\ \Gamma(\Xi_b^{*0}) &= 0.90 \pm 0.16 \pm 0.08\,\mathrm{MeV}, \end{aligned}$$

where the first uncertainties are statistical and the second are systematic. Given these values, those of the other Ξ_b resonances reported previously [16], and the absence of other structures in the δm spectrum, the observed peak is compatible with the $J^P = \frac{3}{2}^+$ state expected in the quark model [2], and we therefore refer to it as the Ξ_b^{*0} baryon.

4 Relative production rate

In addition to the mass and width of the Ξ_b^{*0} state, we measure the rate at which it is produced in the LHCb acceptance relative to the Ξ_b^- baryon. The quantity that is measured is

$$\frac{\sigma(pp \to \Xi_b^{*0} X)\,\mathcal{B}(\Xi_b^{*0} \to \Xi_b^- \pi^+)}{\sigma(pp \to \Xi_b^- X)} = \frac{N(\Xi_b^{*0})}{N(\Xi_b^-)} \frac{1}{\epsilon^{\mathrm{rel}}_{\Xi_b^{*0}}}, \tag{3}$$

where $\epsilon^{\rm rel}_{\Xi_b^{*0}}$ is the ratio of the Ξ_b^{*0} to Ξ_b^- selection efficiencies, and N is a measured yield. Any variation in the ratio of cross-sections $[\sigma(pp \to \Xi_b^{*0} X)] \,/\, \left[\sigma(pp \to \Xi_b^- X)\right]$ between $\sqrt{s} = 7\,\text{TeV}$ and $8\,\text{TeV}$ would be far below the sensitivity of our measurements, and is therefore neglected.

To minimize systematic uncertainties, all aspects of the Ξ_b^- selection are chosen to be common to the inclusive Ξ_b^- and Ξ_b^{*0} samples. Therefore an additional requirement, not applied to the sample used in the mass and width measurements, is imposed that at least one of the Ξ_b^- decay products passes the L0 hadron trigger requirements. The relative efficiency $\epsilon^{\rm rel}_{\Xi_b^{*0}}$ includes the efficiency of detecting the π^+ from the Ξ_b^{*0} decay and the selection criteria imposed on it. It is evaluated using simulated decays, and small corrections (discussed below) are applied to account for residual differences between data and simulation. Including only the uncertainty due to the finite sizes of the simulated samples, the value of $\epsilon^{\rm rel}_{\Xi_b^{*0}}$ is found to be 0.598 ± 0.014.

The yields in data are obtained by fitting the δm and $m_{\rm cand}(\Xi_b^-)$ spectra after applying all selection criteria. For the Ξ_b^{*0} yield, the data are fitted using the same functional form as was used for the full sample. The fit is shown in Fig. 4, and the yield obtained is $N(\Xi_b^{*0}) = 133 \pm 14$. The results of an unbinned, extended maximum likelihood fit to the Ξ_b^- sample are shown in Fig. 5. The shapes used to describe the signal and backgrounds are identical to those described in Ref. [14]. In brief, the signal shape is described by the sum of two Crystal Ball functions [34] with a common mean. The background components are due to misidentified $\Xi_b^- \to \Xi_c^0 K^-$ decays, partially-reconstructed $\Xi_b^- \to \Xi_c^0 \rho^-$ decays, and combinatorial background. The $\Xi_b^- \to \Xi_c^0 K^-$ contribution is also described by the sum of two Crystal Ball functions with a common mean. Its shape parameters are fixed to the values from simulation, and the fractional yield relative to that of $\Xi_b^- \to \Xi_c^0 \pi^-$ is fixed to 3.1%, based on previous studies of this mode [14]. The $\Xi_b^- \to \Xi_c^0 \rho^-$ mass shape is described by an ARGUS function [35], convolved with a Gaussian resolution function. The threshold and shape parameters are fixed based on simulation, and the resolution is fixed to $14\,\text{MeV}/c^2$, the approximate mass resolution for signal decays. The yield is freely varied in the fit. The combinatorial background is described by an exponential function with freely varying shape parameter and yield. To match the criteria used for the Ξ_b^{*0} selection, only Ξ_b^- candidates within $\pm 60\,\text{MeV}/c^2$ of the known mass contribute to the yield, which is found to be $N(\Xi_b^-) = 808 \pm 32$.

Several sources of uncertainty contribute to the production ratio measurement, either in the signal efficiency or in the determination of the yields. Most of the selection requirements are common to both the signal and normalization modes, and therefore the corresponding efficiencies cancel in the production ratio measurement. Effects related to the detection and selection of the π^+ from the Ξ_b^{*0} decay do not cancel, and therefore contribute to the systematic uncertainty. The tracking efficiency is measured using a tag and probe procedure with $J/\psi \to \mu^+\mu^-$ decays [36], and for this momentum range a correction of $(+7.0 \pm 3.0)\%$ is applied. Fit quality requirements on the π^+ track lead to an additional correction of $(-1.5 \pm 1.5)\%$. The simulation is used to estimate the loss of Ξ_b^{*0} efficiency from decays in which the π^+ is reconstructed but has $p_{\rm T} < 100\,\text{MeV}/c$. This loss, 2.7%, is

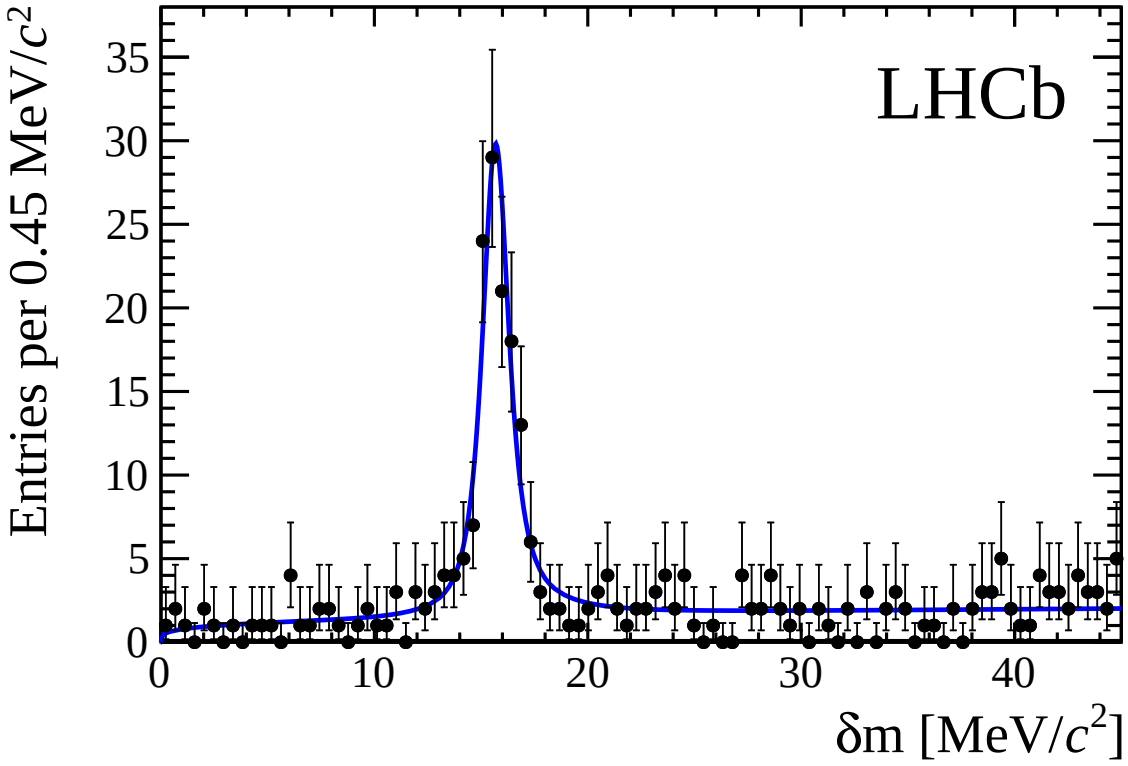

Figure 4: Distribution of δm, using only events in which one or more of the Ξ_b^- decay products pass the L0 hadron trigger requirements. The results of the fit are overlaid.

already included in the efficiency, and does not require an additional correction. Since the simulation reproduces the $p_{\rm T}$ spectrum well for $p_{\rm T} > 100\,{\rm MeV}/c$, we assign half of the value, 1.4%, as a systematic uncertainty associated with the extrapolation to $p_{\rm T} < 100\,{\rm MeV}/c$. Finally, the limited sample sizes of simulated events contribute an uncertainty of 2.4% to the relative efficiency. With these systematic sources included, the relative efficiency is found to be $\epsilon^{\rm rel}_{\Xi_b^{*0}} = 0.598 \pm 0.026$.

For the Ξ_b^{*0} signal yield in data, we assign a 1% systematic uncertainty due to a potential peaking background in which a genuine $\Xi_b^{*0} \to \Xi_b^-\pi^+$, $\Xi_b^- \to \Xi_c^0\pi^-$ decay is found but the Ξ_c^0 is misreconstructed. For the normalization mode, independent variations in the signal and background shapes are investigated, and taken together correspond to a systematic uncertainty in the normalisation mode yield of 2%.

Combining the relative efficiency, the yields, and the systematic uncertainties described above, we find

$$\frac{\sigma(pp \to \Xi_b^{*0} X)\mathcal{B}(\Xi_b^{*0} \to \Xi_b^-\pi^+)}{\sigma(pp \to \Xi_b^- X)} = 0.28 \pm 0.03 \pm 0.01,$$

where the statistical uncertainty takes into account the correlation between $N(\Xi_b^{*0})$ and

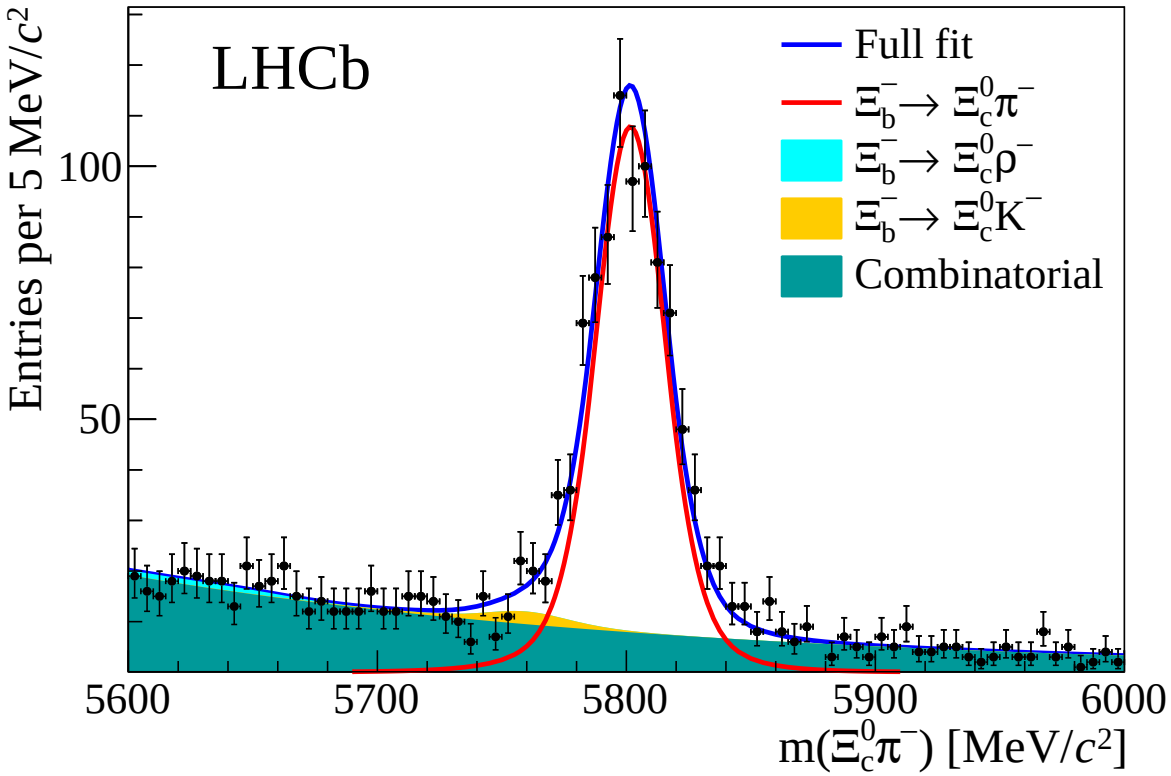

Figure 5: Invariant mass spectrum of selected $\Xi_c^0\pi^-$ candidates. The fit described in the text is overlaid. The Ξ_b^- signal peak and background from combinatorial events are clearly visible, accompanied by small contributions from the peaking background processes $\Xi_b^- \to \Xi_c^0\rho^-$ and $\Xi_b^- \to \Xi_c^0 K^-$.

$N(\Xi_b^-)$.

Table 2: Relative systematic uncertainties on the production ratio.

Effect	Uncertainty
Simulated sample size	2.4%
Tracking efficiency correction	3.0%
Fit quality efficiency correction	1.5%
Soft pion $p_{\rm T}$ cut	1.4%
Ξ_b^{*0} yield	1.0%
Ξ_b^- yield	2.0%
Sum in quadrature	4.9%

5 Summary

Using pp collision data from the LHCb experiment corresponding to an integrated luminosity of $3\,\text{fb}^{-1}$, we observe one highly significant structure in the $\Xi_b^-\pi^+$ mass spectrum near threshold. There is no indication of a second state above the $\Xi_b^-\pi^+$ mass threshold that would indicate the presence of the $\Xi_b^{\prime 0}$ resonance; from this we conclude that $m(\Xi_b^{\prime 0}) \lesssim m(\Xi_b^-) + m(\pi^+)$. The mass difference and width of the Ξ_b^{*0} are measured to be:

$$\begin{aligned} m(\Xi_b^{*0}) - m(\Xi_b^-) - m(\pi^+) &= 15.727 \pm 0.068 \pm 0.023\,\text{MeV}/c^2, \\ \Gamma(\Xi_b^{*0}) &= 0.90 \pm 0.16 \pm 0.08\,\text{MeV}. \end{aligned}$$

We interpret the structure as the $J^P = \frac{3}{2}^+$ Ξ_b^{*0} state observed previously by the CMS collaboration through the decay chain $\Xi_b^{*0} \to \Xi_b^-\pi^+, \Xi_b^- \to J/\psi\,\Xi^-$. Our results are consistent with and about a factor of ten more precise than their measurements, $\delta m = 14.84 \pm 0.74 \pm 0.28\,\text{MeV}/c^2$ and $\Gamma = 2.1 \pm 1.7\,(\text{stat})\,\text{MeV}$ [15]. The measured width of the state is in line with theory expectations: a calculation based on lattice QCD predicted a width of $0.51 \pm 0.16\,\text{MeV}$ [37], and another using the $^3P_0$ model obtained a value of $0.85\,\text{MeV}$ [38].

Combining our measured value for δm with the most precise measured value of the Ξ_b^- mass, $5797.72 \pm 0.46 \pm 0.16 \pm 0.26\,\text{MeV}/c^2$ [14], and the pion mass [28], we obtain

$$m(\Xi_b^{*0}) = 5953.02 \pm 0.07 \pm 0.02 \pm 0.55\,\text{MeV}/c^2,$$

where the third uncertainty is due to the $m(\Xi_b^-)$ measurement. We further combine our result on $\delta m(\Xi_b^{*0})$ with previous LHCb measurements of $\delta m(\Xi_b^{*-}) \equiv m(\Xi_b^0\pi^-) - m(\Xi_b^0) - m(\pi^-) = 23.96 \pm 0.12 \pm 0.06$ MeV/c^2 [16], and of the ground state isospin splitting, $m(\Xi_b^-) - m(\Xi_b^0) = 5.92 \pm 0.60 \pm 0.23\,\text{MeV}/c^2$ [14], to obtain the isospin splitting of the Ξ_b^* states,

$$\begin{aligned} m(\Xi_b^{*-}) - m(\Xi_b^{*0}) &= \delta m(\Xi_b^{*-}) - \delta m(\Xi_b^{*0}) - \left[m(\Xi_b^-) - m(\Xi_b^0)\right] \\ &= 2.31 \pm 0.62 \pm 0.24\,\text{MeV}/c^2. \end{aligned}$$

In combining the above measurements, the systematic uncertainties on the mass scale and the RBW shape are treated as fully correlated between the two δm measurements.

We have also measured the inclusive ratio of production cross-sections to be

$$\frac{\sigma(pp \to \Xi_b^{*0} X)\mathcal{B}(\Xi_b^{*0} \to \Xi_b^-\pi^+)}{\sigma(pp \to \Xi_b^- X)} = 0.28 \pm 0.03 \pm 0.01.$$

This value is similar to the previously measured value from the isospin partner mode, $\Xi_b^{*-} \to \Xi_b^0\pi^-$, of $\dfrac{\sigma(pp \to \Xi_b^{*-} X)\mathcal{B}(\Xi_b^{*-} \to \Xi_b^0\pi^-)}{\sigma(pp \to \Xi_b^0 X)} = 0.21 \pm 0.03 \pm 0.01$ [16]. Taking into account the neutral modes, e.g. $\Xi_b^{*0} \to \Xi_b^0\pi^0$ and $\Xi_b^{*-} \to \Xi_b^-\pi^0$, and contributions from Ξ_b' states [16], it is evident that in pp collisions at 7 and 8 TeV a large fraction of Ξ_b^- and Ξ_b^0 baryons are produced through feed-down from higher-mass states.

Acknowledgements

We express our gratitude to our colleagues in the CERN accelerator departments for the excellent performance of the LHC. We thank the technical and administrative staff at the LHCb institutes. We acknowledge support from CERN and from the national agencies: CAPES, CNPq, FAPERJ and FINEP (Brazil); NSFC (China); CNRS/IN2P3 (France); BMBF, DFG and MPG (Germany); INFN (Italy); FOM and NWO (The Netherlands); MNiSW and NCN (Poland); MEN/IFA (Romania); MinES and FANO (Russia); MinECo (Spain); SNSF and SER (Switzerland); NASU (Ukraine); STFC (United Kingdom); NSF (USA). We acknowledge the computing resources that are provided by CERN, IN2P3 (France), KIT and DESY (Germany), INFN (Italy), SURF (The Netherlands), PIC (Spain), GridPP (United Kingdom), RRCKI and Yandex LLC (Russia), CSCS (Switzerland), IFIN-HH (Romania), CBPF (Brazil), PL-GRID (Poland) and OSC (USA). We are indebted to the communities behind the multiple open source software packages on which we depend. Individual groups or members have received support from AvH Foundation (Germany), EPLANET, Marie Skłodowska-Curie Actions and ERC (European Union), Conseil Général de Haute-Savoie, Labex ENIGMASS and OCEVU, Région Auvergne (France), RFBR and Yandex LLC (Russia), GVA, XuntaGal and GENCAT (Spain), Herchel Smith Fund, The Royal Society, Royal Commission for the Exhibition of 1851 and the Leverhulme Trust (United Kingdom).

References

[1] M. Karliner, B. Keren-Zur, H. J. Lipkin, and J. L. Rosner, *The quark model and b baryons*, Annals Phys. **324** (2009) 2, arXiv:0804.1575.

[2] E. Klempt and J.-M. Richard, *Baryon spectroscopy*, Rev. Mod. Phys. **82** (2010) 1095, arXiv:0901.2055.

[3] R. Lewis and R. M. Woloshyn, *Bottom baryons from a dynamical lattice QCD simulation*, Phys. Rev. **D79** (2009) 014502, arXiv:0806.4783.

[4] D. Ebert, R. N. Faustov, and V. O. Galkin, *Masses of heavy baryons in the relativistic quark model*, Phys. Rev. **D72** (2005) 034026, arXiv:hep-ph/0504112.

[5] X. Liu *et al.*, *Bottom baryons*, Phys. Rev. **D77** (2008) 014031, arXiv:0710.0123.

[6] E. E. Jenkins, *Model-independent bottom baryon mass predictions in the* $1/N_c$ *expansion*, Phys. Rev. **D77** (2008) 034012, arXiv:0712.0406.

[7] M. Karliner, *Heavy quark spectroscopy and prediction of bottom baryon masses*, Nucl. Phys. Proc. Suppl. **187** (2009) 21, arXiv:0806.4951.

[8] J.-R. Zhang and M.-Q. Huang, *Heavy baryon spectroscopy in QCD*, Phys. Rev. **D78** (2008) 094015, arXiv:0811.3266.

[9] Z.-G. Wang, *Analysis of the $\frac{3}{2}^+$ heavy and doubly heavy baryon states with QCD sum rules*, Eur. Phys. J. **C68** (2010) 459, arXiv:1002.2471.

[10] Z. S. Brown, W. Detmold, S. Meinel, and K. Orginos, *Charmed bottom baryon spectroscopy from lattice QCD*, Phys. Rev. **D90** (2014) 094507, arXiv:1409.0497.

[11] A. Valcarce, H. Garcilazo, and J. Vijande, *Towards an understanding of heavy baryon spectroscopy*, Eur. Phys. J. **A37** (2008) 217, arXiv:0807.2973.

[12] A. Limphirat, C. Kobdaj, P. Suebka, and Y. Yan, *Decay widths of ground-state and excited Ξ_b baryons in a nonrelativistic quark model*, Phys. Rev. **C82** (2010) 055201.

[13] LHCb collaboration, R. Aaij *et al.*, *Precision measurement of the mass and lifetime of the Ξ_b^0 baryon*, Phys. Rev. Lett. **113** (2014) 032001, arXiv:1405.7223.

[14] LHCb collaboration, R. Aaij *et al.*, *Precision measurement of the mass and lifetime of the Ξ_b^- baryon*, Phys. Rev. Lett. **113** (2014) 242002, arXiv:1409.8568.

[15] CMS collaboration, S. Chatrchyan *et al.*, *Observation of a new Ξ_b baryon*, Phys. Rev. Lett. **108** (2012) 252002, arXiv:1204.5955.

[16] LHCb collaboration, R. Aaij *et al.*, *Observation of two new Ξ_b^- baryon resonances*, Phys. Rev. Lett. **114** (2015) 062004, arXiv:1411.4849.

[17] LHCb collaboration, A. A. Alves Jr. *et al.*, *The LHCb detector at the LHC*, JINST **3** (2008) S08005.

[18] LHCb collaboration, R. Aaij *et al.*, *LHCb detector performance*, Int. J. Mod. Phys. **A30** (2015) 1530022, arXiv:1412.6352.

[19] R. Aaij *et al.*, *The LHCb trigger and its performance in 2011*, JINST **8** (2013) P04022, arXiv:1211.3055.

[20] V. V. Gligorov and M. Williams, *Efficient, reliable and fast high-level triggering using a bonsai boosted decision tree*, JINST **8** (2013) P02013, arXiv:1210.6861.

[21] T. Sjöstrand, S. Mrenna, and P. Skands, *PYTHIA 6.4 physics and manual*, JHEP **05** (2006) 026, arXiv:hep-ph/0603175; T. Sjöstrand, S. Mrenna, and P. Skands, *A brief introduction to PYTHIA 8.1*, Comput. Phys. Commun. **178** (2008) 852, arXiv:0710.3820.

[22] I. Belyaev *et al.*, *Handling of the generation of primary events in Gauss, the LHCb simulation framework*, J. Phys. Conf. Ser. **331** (2011) 032047.

[23] D. J. Lange, *The EvtGen particle decay simulation package*, Nucl. Instrum. Meth. **A462** (2001) 152.

[24] P. Golonka and Z. Was, *PHOTOS Monte Carlo: A precision tool for QED corrections in Z and W decays*, Eur. Phys. J. **C45** (2006) 97, arXiv:hep-ph/0506026.

[25] Geant4 collaboration, J. Allison *et al.*, *Geant4 developments and applications*, IEEE Trans. Nucl. Sci. **53** (2006) 270; Geant4 collaboration, S. Agostinelli *et al.*, *Geant4: A simulation toolkit*, Nucl. Instrum. Meth. **A506** (2003) 250.

[26] M. Clemencic *et al.*, *The LHCb simulation application, Gauss: Design, evolution and experience*, J. Phys. Conf. Ser. **331** (2011) 032023.

[27] W. D. Hulsbergen, *Decay chain fitting with a Kalman filter*, Nucl. Instrum. Meth. **A552** (2005) 566, arXiv:physics/0503191.

[28] Particle Data Group, K. A. Olive *et al.*, *Review of particle physics*, Chin. Phys. **C38** (2014) 090001, and 2015 update.

[29] J. D. Jackson, *Remarks on the phenomenological analysis of resonances*, Nuovo Cim. **34** (1964) 1644.

[30] J. Blatt and V. Weisskopf, *Theoretical nuclear physics*, John Wiley & Sons, 1952.

[31] LHCb collaboration, R. Aaij *et al.*, *Measurements of the Λ_b^0, Ξ_b^-, and Ω_b^- baryon masses*, Phys. Rev. Lett. **110** (2013) 182001, arXiv:1302.1072.

[32] LHCb collaboration, R. Aaij *et al.*, *Precision measurement of D meson mass differences*, JHEP **06** (2013) 065, arXiv:1304.6865.

[33] BaBar collaboration, J. P. Lees *et al.*, *Measurement of the $D^*(2010)^+$ natural line width and the $D^*(2010)^+ - D^0$ mass difference*, Phys. Rev. **D88** (2013) 052003, Erratum ibid. **D88** (2013) 079902, arXiv:1304.5009; BaBar collaboration, J. P. Lees *et al.*, *Measurement of the $D^*(2010)^+$ meson width and the $D^*(2010)^+ - D^0$ mass difference*, Phys. Rev. Lett. **111** (2013) 111801, Erratum ibid. **111** (2013) 169902, arXiv:1304.5657.

[34] T. Skwarnicki, *A study of the radiative cascade transitions between the Upsilon-prime and Upsilon resonances*, PhD thesis, Institute of Nuclear Physics, Krakow, 1986, DESY-F31-86-02.

[35] ARGUS collaboration, H. Albrecht *et al.*, *Measurement of the polarization in the decay $B \to J/\psi K^*$*, Phys. Lett. **B340** (1994) 217.

[36] LHCb collaboration, R. Aaij *et al.*, *Measurement of the track reconstruction efficiency at LHCb*, JINST **10** (2015) P02007, arXiv:1408.1251.

[37] W. Detmold, C. J. D. Lin, and S. Meinel, *Calculation of the heavy-hadron axial couplings g_1, g_2 and g_3 using lattice QCD*, Phys. Rev. **D85** (2012) 114508, arXiv:1203.3378.

[38] C. Chen *et al.*, *Strong decays of charmed baryons*, Phys. Rev. **D75** (2007) 094017, arXiv:0704.0075.

LHCb collaboration

R. Aaij[39], C. Abellán Beteta[41], B. Adeva[38], M. Adinolfi[47], Z. Ajaltouni[5], S. Akar[6], J. Albrecht[10], F. Alessio[39], M. Alexander[52], S. Ali[42], G. Alkhazov[31], P. Alvarez Cartelle[54], A.A. Alves Jr[58], S. Amato[2], S. Amerio[23], Y. Amhis[7], L. An[3,40], L. Anderlini[18], G. Andreassi[40], M. Andreotti[17,g], J.E. Andrews[59], R.B. Appleby[55], O. Aquines Gutierrez[11], F. Archilli[39], P. d'Argent[12], A. Artamonov[36], M. Artuso[60], E. Aslanides[6], G. Auriemma[26,n], M. Baalouch[5], S. Bachmann[12], J.J. Back[49], A. Badalov[37], C. Baesso[61], S. Baker[54], W. Baldini[17], R.J. Barlow[55], C. Barschel[39], S. Barsuk[7], W. Barter[39], V. Batozskaya[29], V. Battista[40], A. Bay[40], L. Beaucourt[4], J. Beddow[52], F. Bedeschi[24], I. Bediaga[1], L.J. Bel[42], V. Bellee[40], N. Belloli[21,k], I. Belyaev[32], E. Ben-Haim[8], G. Bencivenni[19], S. Benson[39], J. Benton[47], A. Berezhnoy[33], R. Bernet[41], A. Bertolin[23], F. Betti[15], M.-O. Bettler[39], M. van Beuzekom[42], S. Bifani[46], P. Billoir[8], T. Bird[55], A. Birnkraut[10], A. Bizzeti[18,i], T. Blake[49], F. Blanc[40], J. Blouw[11], S. Blusk[60], V. Bocci[26], A. Bondar[35], N. Bondar[31,39], W. Bonivento[16], A. Borgheresi[21,k], S. Borghi[55], M. Borisyak[67], M. Borsato[38], M. Boubdir[9], T.J.V. Bowcock[53], E. Bowen[41], C. Bozzi[17,39], S. Braun[12], M. Britsch[12], T. Britton[60], J. Brodzicka[55], E. Buchanan[47], C. Burr[55], A. Bursche[2], J. Buytaert[39], S. Cadeddu[16], R. Calabrese[17,g], M. Calvi[21,k], M. Calvo Gomez[37,p], P. Campana[19], D. Campora Perez[39], L. Capriotti[55], A. Carbone[15,e], G. Carboni[25,l], R. Cardinale[20,j], A. Cardini[16], P. Carniti[21,k], L. Carson[51], K. Carvalho Akiba[2], G. Casse[53], L. Cassina[21,k], L. Castillo Garcia[40], M. Cattaneo[39], Ch. Cauet[10], G. Cavallero[20], R. Cenci[24,t], M. Charles[8], Ph. Charpentier[39], G. Chatzikonstantinidis[46], M. Chefdeville[4], S. Chen[55], S.-F. Cheung[56], V. Chobanova[38], M. Chrzaszcz[41,27], X. Cid Vidal[39], G. Ciezarek[42], P.E.L. Clarke[51], M. Clemencic[39], H.V. Cliff[48], J. Closier[39], V. Coco[58], J. Cogan[6], E. Cogneras[5], V. Cogoni[16,f], L. Cojocariu[30], G. Collazuol[23,r], P. Collins[39], A. Comerma-Montells[12], A. Contu[39], A. Cook[47], S. Coquereau[8], G. Corti[39], M. Corvo[17,g], B. Couturier[39], G.A. Cowan[51], D.C. Craik[51], A. Crocombe[49], M. Cruz Torres[61], S. Cunliffe[54], R. Currie[54], C. D'Ambrosio[39], E. Dall'Occo[42], J. Dalseno[47], P.N.Y. David[42], A. Davis[58], O. De Aguiar Francisco[2], K. De Bruyn[6], S. De Capua[55], M. De Cian[12], J.M. De Miranda[1], L. De Paula[2], P. De Simone[19], C.-T. Dean[52], D. Decamp[4], M. Deckenhoff[10], L. Del Buono[8], N. Déléage[4], M. Demmer[10], A. Dendek[28], D. Derkach[67], O. Deschamps[5], F. Dettori[39], B. Dey[22], A. Di Canto[39], H. Dijkstra[39], F. Dordei[39], M. Dorigo[40], A. Dosil Suárez[38], A. Dovbnya[44], K. Dreimanis[53], L. Dufour[42], G. Dujany[55], K. Dungs[39], P. Durante[39], R. Dzhelyadin[36], A. Dziurda[39], A. Dzyuba[31], S. Easo[50,39], U. Egede[54], V. Egorychev[32], S. Eidelman[35], S. Eisenhardt[51], U. Eitschberger[10], R. Ekelhof[10], L. Eklund[52], I. El Rifai[5], Ch. Elsasser[41], S. Ely[60], S. Esen[12], H.M. Evans[48], T. Evans[56], A. Falabella[15], C. Färber[39], N. Farley[46], S. Farry[53], R. Fay[53], D. Fazzini[21,k], D. Ferguson[51], V. Fernandez Albor[38], F. Ferrari[15,39], F. Ferreira Rodrigues[1], M. Ferro-Luzzi[39], S. Filippov[34], M. Fiore[17,g], M. Fiorini[17,g], M. Firlej[28], C. Fitzpatrick[40], T. Fiutowski[28], F. Fleuret[7,b], K. Fohl[39], M. Fontana[16], F. Fontanelli[20,j], D. C. Forshaw[60], R. Forty[39], M. Frank[39], C. Frei[39], M. Frosini[18], J. Fu[22], E. Furfaro[25,l], A. Gallas Torreira[38], D. Galli[15,e], S. Gallorini[23], S. Gambetta[51], M. Gandelman[2], P. Gandini[56], Y. Gao[3], J. García Pardiñas[38], J. Garra Tico[48], L. Garrido[37], P.J. Garsed[48], D. Gascon[37], C. Gaspar[39], L. Gavardi[10], G. Gazzoni[5], D. Gerick[12], E. Gersabeck[12], M. Gersabeck[55], T. Gershon[49], Ph. Ghez[4], S. Gianì[40], V. Gibson[48], O.G. Girard[40], L. Giubega[30], V.V. Gligorov[39], C. Göbel[61], D. Golubkov[32], A. Golutvin[54,39], A. Gomes[1,a], C. Gotti[21,k], M. Grabalosa Gándara[5], R. Graciani Diaz[37], L.A. Granado Cardoso[39], E. Graugés[37], E. Graverini[41], G. Graziani[18], A. Grecu[30], P. Griffith[46], L. Grillo[12], O. Grünberg[65], E. Gushchin[34], Yu. Guz[36,39], T. Gys[39], T. Hadavizadeh[56], C. Hadjivasiliou[60], G. Haefeli[40],

C. Haen[39], S.C. Haines[48], S. Hall[54], B. Hamilton[59], X. Han[12], S. Hansmann-Menzemer[12], N. Harnew[56], S.T. Harnew[47], J. Harrison[55], J. He[39], T. Head[40], A. Heister[9], K. Hennessy[53], P. Henrard[5], L. Henry[8], J.A. Hernando Morata[38], E. van Herwijnen[39], M. Heß[65], A. Hicheur[2], D. Hill[56], M. Hoballah[5], C. Hombach[55], L. Hongming[40], W. Hulsbergen[42], T. Humair[54], M. Hushchyn[67], N. Hussain[56], D. Hutchcroft[53], M. Idzik[28], P. Ilten[57], R. Jacobsson[39], A. Jaeger[12], J. Jalocha[56], E. Jans[42], A. Jawahery[59], M. John[56], D. Johnson[39], C.R. Jones[48], C. Joram[39], B. Jost[39], N. Jurik[60], S. Kandybei[44], W. Kanso[6], M. Karacson[39], T.M. Karbach[39,†], S. Karodia[52], M. Kecke[12], M. Kelsey[60], I.R. Kenyon[46], M. Kenzie[39], T. Ketel[43], E. Khairullin[67], B. Khanji[21,39,k], C. Khurewathanakul[40], T. Kirn[9], S. Klaver[55], K. Klimaszewski[29], M. Kolpin[12], I. Komarov[40], R.F. Koopman[43], P. Koppenburg[42], M. Kozeiha[5], L. Kravchuk[34], K. Kreplin[12], M. Kreps[49], P. Krokovny[35], F. Kruse[10], W. Krzemien[29], W. Kucewicz[27,o], M. Kucharczyk[27], V. Kudryavtsev[35], A. K. Kuonen[40], K. Kurek[29], T. Kvaratskheliya[32], D. Lacarrere[39], G. Lafferty[55,39], A. Lai[16], D. Lambert[51], G. Lanfranchi[19], C. Langenbruch[49], B. Langhans[39], T. Latham[49], C. Lazzeroni[46], R. Le Gac[6], J. van Leerdam[42], J.-P. Lees[4], R. Lefèvre[5], A. Leflat[33,39], J. Lefrançois[7], F. Lemaitre[39], E. Lemos Cid[38], O. Leroy[6], T. Lesiak[27], B. Leverington[12], Y. Li[7], T. Likhomanenko[67,66], R. Lindner[39], C. Linn[39], F. Lionetto[41], B. Liu[16], X. Liu[3], D. Loh[49], I. Longstaff[52], J.H. Lopes[2], D. Lucchesi[23,r], M. Lucio Martinez[38], H. Luo[51], A. Lupato[23], E. Luppi[17,g], O. Lupton[56], N. Lusardi[22], A. Lusiani[24], X. Lyu[62], F. Machefert[7], F. Maciuc[30], O. Maev[31], K. Maguire[55], S. Malde[56], A. Malinin[66], G. Manca[7], G. Mancinelli[6], P. Manning[60], A. Mapelli[39], J. Maratas[5], J.F. Marchand[4], U. Marconi[15], C. Marin Benito[37], P. Marino[24,t], J. Marks[12], G. Martellotti[26], M. Martin[6], M. Martinelli[40], D. Martinez Santos[38], F. Martinez Vidal[68], D. Martins Tostes[2], L.M. Massacrier[7], A. Massafferri[1], R. Matev[39], A. Mathad[49], Z. Mathe[39], C. Matteuzzi[21], A. Mauri[41], B. Maurin[40], A. Mazurov[46], M. McCann[54], J. McCarthy[46], A. McNab[55], R. McNulty[13], B. Meadows[58], F. Meier[10], M. Meissner[12], D. Melnychuk[29], M. Merk[42], A Merli[22,u], E Michielin[23], D.A. Milanes[64], M.-N. Minard[4], D.S. Mitzel[12], J. Molina Rodriguez[61], I.A. Monroy[64], S. Monteil[5], M. Morandin[23], P. Morawski[28], A. Mordà[6], M.J. Morello[24,t], J. Moron[28], A.B. Morris[51], R. Mountain[60], F. Muheim[51], MM Mulder[42], D. Müller[55], J. Müller[10], K. Müller[41], V. Müller[10], M. Mussini[15], B. Muster[40], P. Naik[47], T. Nakada[40], R. Nandakumar[50], A. Nandi[56], I. Nasteva[2], M. Needham[51], N. Neri[22], S. Neubert[12], N. Neufeld[39], M. Neuner[12], A.D. Nguyen[40], C. Nguyen-Mau[40,q], V. Niess[5], S. Nieswand[9], R. Niet[10], N. Nikitin[33], T. Nikodem[12], A. Novoselov[36], D.P. O'Hanlon[49], A. Oblakowska-Mucha[28], V. Obraztsov[36], S. Ogilvy[19], O. Okhrimenko[45], R. Oldeman[16,48,f], C.J.G. Onderwater[69], B. Osorio Rodrigues[1], J.M. Otalora Goicochea[2], A. Otto[39], P. Owen[54], A. Oyanguren[68], A. Palano[14,d], F. Palombo[22,u], M. Palutan[19], J. Panman[39], A. Papanestis[50], M. Pappagallo[52], L.L. Pappalardo[17,g], C. Pappenheimer[58], W. Parker[59], C. Parkes[55], G. Passaleva[18], G.D. Patel[53], M. Patel[54], C. Patrignani[20,j], A. Pearce[55,50], A. Pellegrino[42], G. Penso[26,m], M. Pepe Altarelli[39], S. Perazzini[39], P. Perret[5], L. Pescatore[46], K. Petridis[47], A. Petrolini[20,j], M. Petruzzo[22], E. Picatoste Olloqui[37], B. Pietrzyk[4], M. Pikies[27], D. Pinci[26], A. Pistone[20], A. Piucci[12], S. Playfer[51], M. Plo Casasus[38], T. Poikela[39], F. Polci[8], A. Poluektov[49,35], I. Polyakov[32], E. Polycarpo[2], A. Popov[36], D. Popov[11,39], B. Popovici[30], C. Potterat[2], E. Price[47], J.D. Price[53], J. Prisciandaro[38], A. Pritchard[53], C. Prouve[47], V. Pugatch[45], A. Puig Navarro[40], G. Punzi[24,s], W. Qian[56], R. Quagliani[7,47], B. Rachwal[27], J.H. Rademacker[47], M. Rama[24], M. Ramos Pernas[38], M.S. Rangel[2], I. Raniuk[44], G. Raven[43], F. Redi[54], S. Reichert[10], A.C. dos Reis[1], V. Renaudin[7], S. Ricciardi[50], S. Richards[47], M. Rihl[39], K. Rinnert[53,39], V. Rives Molina[37], P. Robbe[7], A.B. Rodrigues[1], E. Rodrigues[58], J.A. Rodriguez Lopez[64], P. Rodriguez Perez[55],

A. Rogozhnikov[67], S. Roiser[39], V. Romanovsky[36], A. Romero Vidal[38], J. W. Ronayne[13], M. Rotondo[23], T. Ruf[39], P. Ruiz Valls[68], J.J. Saborido Silva[38], N. Sagidova[31], B. Saitta[16,f], V. Salustino Guimaraes[2], C. Sanchez Mayordomo[68], B. Sanmartin Sedes[38], R. Santacesaria[26], C. Santamarina Rios[38], M. Santimaria[19], E. Santovetti[25,l], A. Sarti[19,m], C. Satriano[26,n], A. Satta[25], D.M. Saunders[47], D. Savrina[32,33], S. Schael[9], M. Schiller[39], H. Schindler[39], M. Schlupp[10], M. Schmelling[11], T. Schmelzer[10], B. Schmidt[39], O. Schneider[40], A. Schopper[39], M. Schubiger[40], M.-H. Schune[7], R. Schwemmer[39], B. Sciascia[19], A. Sciubba[26,m], A. Semennikov[32], A. Sergi[46], N. Serra[41], J. Serrano[6], L. Sestini[23], P. Seyfert[21], M. Shapkin[36], I. Shapoval[17,44,g], Y. Shcheglov[31], T. Shears[53], L. Shekhtman[35], V. Shevchenko[66], A. Shires[10], B.G. Siddi[17], R. Silva Coutinho[41], L. Silva de Oliveira[2], G. Simi[23,s], M. Sirendi[48], N. Skidmore[47], T. Skwarnicki[60], E. Smith[54], I.T. Smith[51], J. Smith[48], M. Smith[55], H. Snoek[42], M.D. Sokoloff[58], F.J.P. Soler[52], F. Soomro[40], D. Souza[47], B. Souza De Paula[2], B. Spaan[10], P. Spradlin[52], S. Sridharan[39], F. Stagni[39], M. Stahl[12], S. Stahl[39], S. Stefkova[54], O. Steinkamp[41], O. Stenyakin[36], S. Stevenson[56], S. Stoica[30], S. Stone[60], B. Storaci[41], S. Stracka[24,t], M. Straticiuc[30], U. Straumann[41], L. Sun[58], W. Sutcliffe[54], K. Swientek[28], S. Swientek[10], V. Syropoulos[43], M. Szczekowski[29], T. Szumlak[28], S. T'Jampens[4], A. Tayduganov[6], T. Tekampe[10], G. Tellarini[17,g], F. Teubert[39], C. Thomas[56], E. Thomas[39], J. van Tilburg[42], V. Tisserand[4], M. Tobin[40], S. Tolk[43], L. Tomassetti[17,g], D. Tonelli[39], S. Topp-Joergensen[56], E. Tournefier[4], S. Tourneur[40], K. Trabelsi[40], M. Traill[52], M.T. Tran[40], M. Tresch[41], A. Trisovic[39], A. Tsaregorodtsev[6], P. Tsopelas[42], N. Tuning[42,39], A. Ukleja[29], A. Ustyuzhanin[67,66], U. Uwer[12], C. Vacca[16,39,f], V. Vagnoni[15,39], S. Valat[39], G. Valenti[15], A. Vallier[7], R. Vazquez Gomez[19], P. Vazquez Regueiro[38], C. Vázquez Sierra[38], S. Vecchi[17], M. van Veghel[42], J.J. Velthuis[47], M. Veltri[18,h], G. Veneziano[40], M. Vesterinen[12], B. Viaud[7], D. Vieira[2], M. Vieites Diaz[38], X. Vilasis-Cardona[37,p], V. Volkov[33], A. Vollhardt[41], D. Voong[47], A. Vorobyev[31], V. Vorobyev[35], C. Voß[65], J.A. de Vries[42], R. Waldi[65], C. Wallace[49], R. Wallace[13], J. Walsh[24], J. Wang[60], D.R. Ward[48], N.K. Watson[46], D. Websdale[54], A. Weiden[41], M. Whitehead[39], J. Wicht[49], G. Wilkinson[56,39], M. Wilkinson[60], M. Williams[39], M.P. Williams[46], M. Williams[57], T. Williams[46], F.F. Wilson[50], J. Wimberley[59], J. Wishahi[10], W. Wislicki[29], M. Witek[27], G. Wormser[7], S.A. Wotton[48], K. Wraight[52], S. Wright[48], K. Wyllie[39], Y. Xie[63], Z. Xu[40], Z. Yang[3], H. Yin[63], J. Yu[63], X. Yuan[35], O. Yushchenko[36], M. Zangoli[15], M. Zavertyaev[11,c], L. Zhang[3], Y. Zhang[7], A. Zhelezov[12], Y. Zheng[62], A. Zhokhov[32], L. Zhong[3], V. Zhukov[9], S. Zucchelli[15].

[1] *Centro Brasileiro de Pesquisas Físicas (CBPF), Rio de Janeiro, Brazil*
[2] *Universidade Federal do Rio de Janeiro (UFRJ), Rio de Janeiro, Brazil*
[3] *Center for High Energy Physics, Tsinghua University, Beijing, China*
[4] *LAPP, Université Savoie Mont-Blanc, CNRS/IN2P3, Annecy-Le-Vieux, France*
[5] *Clermont Université, Université Blaise Pascal, CNRS/IN2P3, LPC, Clermont-Ferrand, France*
[6] *CPPM, Aix-Marseille Université, CNRS/IN2P3, Marseille, France*
[7] *LAL, Université Paris-Sud, CNRS/IN2P3, Orsay, France*
[8] *LPNHE, Université Pierre et Marie Curie, Université Paris Diderot, CNRS/IN2P3, Paris, France*
[9] *I. Physikalisches Institut, RWTH Aachen University, Aachen, Germany*
[10] *Fakultät Physik, Technische Universität Dortmund, Dortmund, Germany*
[11] *Max-Planck-Institut für Kernphysik (MPIK), Heidelberg, Germany*
[12] *Physikalisches Institut, Ruprecht-Karls-Universität Heidelberg, Heidelberg, Germany*
[13] *School of Physics, University College Dublin, Dublin, Ireland*
[14] *Sezione INFN di Bari, Bari, Italy*
[15] *Sezione INFN di Bologna, Bologna, Italy*

[16] *Sezione INFN di Cagliari, Cagliari, Italy*
[17] *Sezione INFN di Ferrara, Ferrara, Italy*
[18] *Sezione INFN di Firenze, Firenze, Italy*
[19] *Laboratori Nazionali dell'INFN di Frascati, Frascati, Italy*
[20] *Sezione INFN di Genova, Genova, Italy*
[21] *Sezione INFN di Milano Bicocca, Milano, Italy*
[22] *Sezione INFN di Milano, Milano, Italy*
[23] *Sezione INFN di Padova, Padova, Italy*
[24] *Sezione INFN di Pisa, Pisa, Italy*
[25] *Sezione INFN di Roma Tor Vergata, Roma, Italy*
[26] *Sezione INFN di Roma La Sapienza, Roma, Italy*
[27] *Henryk Niewodniczanski Institute of Nuclear Physics Polish Academy of Sciences, Kraków, Poland*
[28] *AGH - University of Science and Technology, Faculty of Physics and Applied Computer Science, Kraków, Poland*
[29] *National Center for Nuclear Research (NCBJ), Warsaw, Poland*
[30] *Horia Hulubei National Institute of Physics and Nuclear Engineering, Bucharest-Magurele, Romania*
[31] *Petersburg Nuclear Physics Institute (PNPI), Gatchina, Russia*
[32] *Institute of Theoretical and Experimental Physics (ITEP), Moscow, Russia*
[33] *Institute of Nuclear Physics, Moscow State University (SINP MSU), Moscow, Russia*
[34] *Institute for Nuclear Research of the Russian Academy of Sciences (INR RAN), Moscow, Russia*
[35] *Budker Institute of Nuclear Physics (SB RAS) and Novosibirsk State University, Novosibirsk, Russia*
[36] *Institute for High Energy Physics (IHEP), Protvino, Russia*
[37] *Universitat de Barcelona, Barcelona, Spain*
[38] *Universidad de Santiago de Compostela, Santiago de Compostela, Spain*
[39] *European Organization for Nuclear Research (CERN), Geneva, Switzerland*
[40] *Ecole Polytechnique Fédérale de Lausanne (EPFL), Lausanne, Switzerland*
[41] *Physik-Institut, Universität Zürich, Zürich, Switzerland*
[42] *Nikhef National Institute for Subatomic Physics, Amsterdam, The Netherlands*
[43] *Nikhef National Institute for Subatomic Physics and VU University Amsterdam, Amsterdam, The Netherlands*
[44] *NSC Kharkiv Institute of Physics and Technology (NSC KIPT), Kharkiv, Ukraine*
[45] *Institute for Nuclear Research of the National Academy of Sciences (KINR), Kyiv, Ukraine*
[46] *University of Birmingham, Birmingham, United Kingdom*
[47] *H.H. Wills Physics Laboratory, University of Bristol, Bristol, United Kingdom*
[48] *Cavendish Laboratory, University of Cambridge, Cambridge, United Kingdom*
[49] *Department of Physics, University of Warwick, Coventry, United Kingdom*
[50] *STFC Rutherford Appleton Laboratory, Didcot, United Kingdom*
[51] *School of Physics and Astronomy, University of Edinburgh, Edinburgh, United Kingdom*
[52] *School of Physics and Astronomy, University of Glasgow, Glasgow, United Kingdom*
[53] *Oliver Lodge Laboratory, University of Liverpool, Liverpool, United Kingdom*
[54] *Imperial College London, London, United Kingdom*
[55] *School of Physics and Astronomy, University of Manchester, Manchester, United Kingdom*
[56] *Department of Physics, University of Oxford, Oxford, United Kingdom*
[57] *Massachusetts Institute of Technology, Cambridge, MA, United States*
[58] *University of Cincinnati, Cincinnati, OH, United States*
[59] *University of Maryland, College Park, MD, United States*
[60] *Syracuse University, Syracuse, NY, United States*
[61] *Pontifícia Universidade Católica do Rio de Janeiro (PUC-Rio), Rio de Janeiro, Brazil, associated to* [2]
[62] *University of Chinese Academy of Sciences, Beijing, China, associated to* [3]
[63] *Institute of Particle Physics, Central China Normal University, Wuhan, Hubei, China, associated to* [3]
[64] *Departamento de Fisica , Universidad Nacional de Colombia, Bogota, Colombia, associated to* [8]
[65] *Institut für Physik, Universität Rostock, Rostock, Germany, associated to* [12]

[66] National Research Centre Kurchatov Institute, Moscow, Russia, associated to [32]
[67] Yandex School of Data Analysis, Moscow, Russia, associated to [32]
[68] Instituto de Fisica Corpuscular (IFIC), Universitat de Valencia-CSIC, Valencia, Spain, associated to [37]
[69] Van Swinderen Institute, University of Groningen, Groningen, The Netherlands, associated to [42]

[a] Universidade Federal do Triângulo Mineiro (UFTM), Uberaba-MG, Brazil
[b] Laboratoire Leprince-Ringuet, Palaiseau, France
[c] P.N. Lebedev Physical Institute, Russian Academy of Science (LPI RAS), Moscow, Russia
[d] Università di Bari, Bari, Italy
[e] Università di Bologna, Bologna, Italy
[f] Università di Cagliari, Cagliari, Italy
[g] Università di Ferrara, Ferrara, Italy
[h] Università di Urbino, Urbino, Italy
[i] Università di Modena e Reggio Emilia, Modena, Italy
[j] Università di Genova, Genova, Italy
[k] Università di Milano Bicocca, Milano, Italy
[l] Università di Roma Tor Vergata, Roma, Italy
[m] Università di Roma La Sapienza, Roma, Italy
[n] Università della Basilicata, Potenza, Italy
[o] AGH - University of Science and Technology, Faculty of Computer Science, Electronics and Telecommunications, Kraków, Poland
[p] LIFAELS, La Salle, Universitat Ramon Llull, Barcelona, Spain
[q] Hanoi University of Science, Hanoi, Viet Nam
[r] Università di Padova, Padova, Italy
[s] Università di Pisa, Pisa, Italy
[t] Scuola Normale Superiore, Pisa, Italy
[u] Università degli Studi di Milano, Milano, Italy

[†] Deceased